

Quantitative Characterization of RCA-Based DNA Hydrogels – Towards Rational Materials Design

Svenja A. Moench,^[a] Phillip Lemke,^[a] Julia Weisser,^[a] Iliya D. Stoev,^[b] Kersten S. Rabe,^[a] Carmen M. Domínguez,^[a] and Christof M. Niemeyer^{*[a]}

DNA hydrogels hold significant promise for biomedical applications and can be synthesized through enzymatic Rolling Circle Amplification (RCA). Due to the exploratory nature of this emerging field, standardized RCA protocols specifying the impact of reaction parameters are currently lacking. This study varied template sequences and reagent concentrations, evaluating RCA synthesis efficiency and hydrogel mechanical properties through quantitative PCR (qPCR) and indentation measurements, respectively. Primer concentration and stabilizing additives showed minimal impact on RCA efficiency, while changes in polymerase and nucleotide concentrations had a

stronger effect. Concentration of the circular template exerted the greatest influence on RCA productivity. An exponential correlation between hydrogel viscosity and DNA amplicon concentration was observed, with nucleobase sequence significantly affecting both amplification efficiency and material properties, particularly through secondary structures. This study suggests that combining high-throughput experimental methods with structural folding prediction offers a viable approach for systematically establishing structure-property relationships, aiding the rational design of DNA hydrogel material systems.

Introduction

DNA hydrogels, with their biocompatibility, stimuli-responsiveness, and programmable structures, have emerged in recent years as promising candidates for diverse applications, such as drug delivery, tissue engineering, and biosensing.^[1] A widely used method for the production of DNA hydrogels with varying structural and morphological properties is based on rolling circle amplification (RCA),^[2] in which the DNA-dependent phi29 polymerase extends a short oligonucleotide primer along a circular template in an isothermal and cost-effective enzymatic synthesis protocol. By displacing the downstream strand, the circular template is continuously extended without the phi29 polymerase detaching from the template and long single-stranded DNA (ssDNA) concatemers (>20,000 bases) are formed.^[3] The formation of intra- and intermolecular hydrogen bonds and physical entanglement of the single-stranded amplicons then results in very soft polymer materials whose

properties vary depending on the degree of drying, DNA and water content, ranging from non-Newtonian viscous liquids to soft and even tough hydrogels.

Due to its ease of implementation and high amplification rates, the RCA method is used extensively in biosensing and biomedical diagnostics, where it is employed in amplification reactions for the detection of DNA sequences.^[4] For certain analytical applications, the experimental process parameters for performing RCA, such as reagent concentrations, reaction temperature and time, can be tightly regulated and even summarized into standard operating procedures (SOPs), as the circular template for RCA is usually fixed. Such SOPs cannot be specified for the use of RCA for the production of new materials, as this young field of research is still characterized by exploratory studies in which, for example, tailor-made material properties are to be generated by variation in the template sequence or post-synthetic modification. The literature therefore contains a large number of protocols for RCA-based material synthesis which, in addition to the use of different template sequences, also differ considerably in some cases in basic process parameters, such as the preparation and concentration of the circular template, the quantity and concentration of primer and enzyme or the addition of additives (e.g. bovine serum albumin, BSA). In particular, the influence of the sequence of the circular template, such as GC content and specific sequence of nucleotide building blocks, on the efficiency of the RCA and the material properties of the resulting hydrogels has hardly been systematically investigated.^[5] It is thus unclear whether the variation of the above-mentioned process parameters has a different effect on different template sequences. This lack of clarity as to which parameters in the template sequence and RCA protocol design contribute to processivity of enzymatic amplification and/or altered materials properties,^[5b] is not only a challenge for the

[a] S. A. Moench, P. Lemke, J. Weisser, K. S. Rabe, C. M. Domínguez, C. M. Niemeyer
Institute for Biological Interfaces (IBG-1), Karlsruhe Institute of Technology (KIT), Hermann-von-Helmholtz Platz 1, Eggenstein-Leopoldshafen 76344, Germany
E-mail: niemeyer@kit.edu

[b] I. D. Stoev
Institute of Biological and Chemical Systems - Biophysical Information Processing (IBCS-BIP), Karlsruhe Institute of Technology (KIT), Hermann-von-Helmholtz Platz 1, Eggenstein-Leopoldshafen 76344, Germany

Supporting information for this article is available on the WWW under <https://doi.org/10.1002/chem.202401788>

© 2024 The Author(s). Chemistry - A European Journal published by Wiley-VCH GmbH. This is an open access article under the terms of the Creative Commons Attribution Non-Commercial NoDerivs License, which permits use and distribution in any medium, provided the original work is properly cited, the use is non-commercial and no modifications or adaptations are made.

advancement of the research field to enable the rational design and tailored material properties of RCA-based DNA hydrogels, it also hinders our fundamental understanding of the RCA process.

In this work, we aim to address the aforementioned problem of the lack of rationality of RCA-based materials synthesis by performing, for the first time, a systematic analysis of the critical process parameters. For this purpose, the influence of the reagent concentration (template, primer, enzyme, additives) on the DNA amplification efficiency and the material properties of the formed hydrogels was investigated using different template sequences. Combining the experimental results with the structural folding prediction of the RCA-produced amplicons using the web server mfold allowed the identification of key parameters and provided first valuable insights into the underlying molecular mechanisms. The approach introduced here lays a solid foundation and an initial step towards establishing systematic sequence-structure-property relationships, serving as a basis for the rational design of DNA hydrogel materials systems.

Results and Discussion

To address the problem of the lack of standardization of RCA-based material synthesis, we aimed to perform a systematic analysis of various process parameters, in particular the

influence of the concentration of template, primer, enzyme and any additives on the DNA amplification efficiency and the material properties of the hydrogels formed. For this purpose, we initially selected three template sequences that are well-described in the literature and differ in their DNA sequence and thus in their ability to form secondary structures by intramolecular base pairing. The sequences of templates A and B were designed by the Walther group for the preparation of mechanosensitive RCA hydrogels.^[6] Sequence C, which was originally designed by the Tan group for the synthesis of DNA hydrogel-based “nanoflowers”^[7] and used by us for the preparation of DNA nanocomposite materials,^[8] contains stem loops and restriction sites for the purpose of applications in drug delivery and cell culture. Furthermore, the experimental protocols of RCA synthesis according to Walther and Tan differ significantly, especially in the concentration of template, primer, enzyme and BSA addition (Figure 1), with higher concentrations of each reaction component and BSA added in the Tan protocol than in the Walther protocol, with the exception of dNTPs. These differences should allow us to assess the influence of the different parameters on the amount of amplified RCA product and their mechanical properties. The template sequences used in this study differ in length, GC content and in the proportions of hairpins or other forms of secondary structures occurring in the RCA-formed amplicon concatemers (Figure S1). A detailed overview of all DNA sequences and RCA protocols used here can be found in Tables S1–S3.

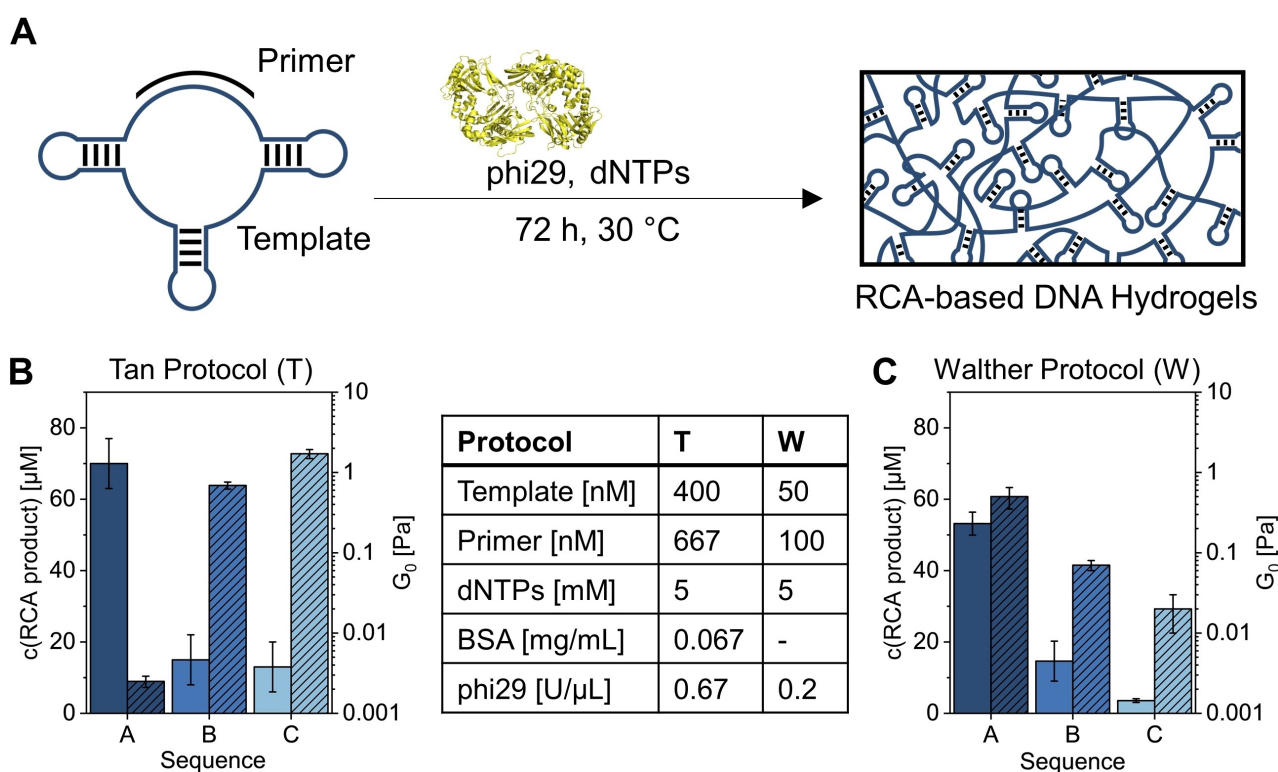







Figure 1. Synthesis and characterization of Rolling Circle Amplification (RCA)-based DNA hydrogels. (A) Schematics of RCA hydrogel synthesis. DNA hydrogels form through elongation of an oligonucleotide primer to single-stranded DNA concatemers via replication of a circular template, resulting in entangled long DNA strands (> 20,000 bases). (B, C): RCA product concentration (filled bars) and mechanical properties (hatched bars) of hydrogels obtained from sequences (A–C) prepared with different reagent concentrations (Table) according to the RCA protocols by Tan (B) or Walther (C). Note the logarithmic scale for the mechanical characterization on the right y-axes in (B) and (C).

To experimentally investigate the influence of reagent concentrations, hydrogels with sequences A–C were synthesized according to either Tan's^[7] (Figure 1B) or Walther's,^[6] protocol (Figure 1C). Sequence A has the smallest amount and sequence C has the highest amount of secondary structures (Figure S1). The reaction time for all RCA reactions was kept at 72 h at 30 °C, as the amplified DNA concentration reached its plateau phase and endpoint values could be determined.^[5b] A detailed overview of the protocols can be found in Table S1. Quantitative polymerase chain reaction (qPCR) was used to determine the RCA product concentration in the hydrogels in order to quantify the concentration of amplicons in the formed hydrogels.^[5b] In brief, aliquots of RCA samples were diluted, briefly sonicated to induce fragmentation of the long ssDNA concatemers, and then quantified by qPCR using external calibration curves. The mechanical properties of the hydrogels were analyzed using rotational rheometry. The elastic plateau modulus (G_0) was used for comparative analysis of gel elasticity. G_0 quantifies the storage modulus G' in the range where G' is independent of the oscillation frequency and is a measure of the elasticity of the sample.^[9]

The data shown in Figure 1B^[10] and C^[5b] clearly demonstrate that the reagent concentration has a strong influence on both the quantity and the material properties of the RCA product. It is also evident that the material properties do not correlate directly with the amount of DNA polymer. Specifically, in the case of templates A and C, the Tan protocol (Figure 1B) led to greater RCA product amplification than the Walther protocol (Figure 1C). Interestingly, the mechanical properties of the latter show a positive correlation with the DNA concentration (the more DNA polymer, the higher G_0), while a negative correlation is observed for the DNA materials produced with the Tan protocol. This direct comparison of the synthesis protocols can be seen as a clear indication that the amount of secondary structures formed can have a greater influence than the actual amount of DNA (Figure S1).

However, our understanding of the formation and properties of these complex DNA materials is currently still very limited. For instance, the role of the nucleotide sequence of the template (here sequences A, B and C), which directly influences both the enzymatic amplification and the intra- and intermolecular interactions of the formed DNA chains, is not yet understood. To address these challenges through a more rational design and determine previously unknown sequence-property relationships, we opted for a new template system. Since the aforementioned sequences A–C display significant variations in length, nucleotide composition and secondary structure formation (Figure S1), and since these factors are suggested to strongly influence the synthesis efficiency and material properties,^[5b] we designed a template system consisting of sequences that have identical lengths and GC composition, but a different propensity to form secondary structures. Specifically, we designed five different templates with a length of 96 nucleotides (nt) and a GC content of 60.4%, whose simulated complementary amplicon products have zero (sequence D0), one (D1), two (D2) or three hairpin loops (D3a, D3b) in the predicted secondary structures (Table 1). The

Table 1. Overview of designed template sequences D0–3, including the predicted folding for one amplicon unit, length of the template, GC content, number of hairpins, percentage of bases in secondary structures of amplicon and the Gibbs free energy (ΔG) of the folded amplicon structure.

Sequence	D0	D1	D2	D3a	D3b
Structure*					
Length [nt]	96	96	96	96	96
GC Content [%]	60.4	60.4	60.4	60.4	60.4
Count of Hairpins	0	1	2	3	3
% of Bases in Secondary Structures ^[a]	0	21	42	56	63
ΔG [kcal/mol]*	0	−10.04	−25.36	−29.19	−35.59

[a] determined by simulation using the mfold web server.^[11]

simulations were performed with the webserver mfold for the linear amplicon unit. Since the simulations of contiguous amplicon concatemers (Figure S2) showed that slight sequence variations of template D3a resulted in strong effects on the formation of secondary structures, the additional sequence D3b was included to allow mechanistic conclusions.

To enable the RCA experiments, the linear template oligonucleotides were circularized by hybridizing them with the bridging primer and linking the ends using T4 ligase (Figure S3). The reaction mixture was then subjected to ExoI/ExoIII exonuclease digestion to remove all linear DNA fragments. The remaining DNA fragments were purified by ultrafiltration and analyzed by Urea-PAGE (Figure S3B). Determination of the ligation efficiency by UV/Vis absorbance measurements resulted in a uniform value of about 20–25% for all sequences (Figure S3C). However, close inspection of the Urea-PAGE analysis revealed only very faint bands of both the linear or circularized oligonucleotides of template D0. This may be due to the numerous consecutive guanine residues present in the sequence, as it is known that such oligonucleotides are difficult to synthesize.^[12]

To experimentally investigate changes in DNA conformation induced by the introduction of up to three hairpin structures, we performed circular dichroism (CD) spectroscopy^[13] with the linear and circularized templates D0–D3 (Figure S4). All spectra showed the characteristic peaks of the B-DNA conformation, with spectroscopic evidence for the presence of guanine quadruplex structures being observable for templates D0 and D1, which contain a high number of consecutive guanine bases. Comparison of the peak signal intensities of the linear and circularized templates suggested changes in base stacking that could be due to differences in helical twisting, e.g. due to supercoiled conformation of the circular DNA. Preliminary tests for RCA using the linear template showed, as expected, that only very small amounts of polymeric RCA product were formed

(Figure S5) thus underscoring the need for circularized templates for the RCA process. In contrast, when circularized templates were used with both the Tan and Walther protocols, clear product formation was observed for all template sequences even by simple electrophoretic analysis (Figure S6). The only exception was sequence D0, where no product formation was observed under Walther conditions, presumably due to the insufficient sensitivity of gel electrophoresis.

For a more detailed investigation, quantification of the RCA products was performed by qPCR using the previously established method (for representative calibration curves, see Figure S7).^[5b] In order to rapidly characterize the mechanical properties of the resulting products and with high throughput, we used a recently developed in-house indentation platform,^[10] which allows us to quantify apparent viscosity ($Visc_{Ap}$) of particularly soft and viscous DNA hydrogels. The determination of apparent viscosity is common in research and development, especially for the characterization of non-Newtonian fluids.^[14]

The results obtained for the RCA of the D sequences using the Tan and Walther protocols are shown in Figures 2A and B, respectively. We obtained consistently 5–10 times more RCA product with the Tan protocol than with the Walther protocol (filled bars in Figure 2), leading to product concentrations in the 100- μ M range. However, the relative synthesis efficiency for the different D materials was very similar for both protocols and increased from D0 to D3a. Template D3b, whose amplicon concatemers show a higher tendency to form secondary structures than D3a (Figure S2), revealed a notably lower amplification efficiency than D3a, suggesting that intramolecular folding of the amplicon concatemers has a strong influence on the productivity of the RCA.^[15] Also, the D0 template led to very low concentrations in the <1- μ M range with also a very low apparent viscosity. In addition to the low purity of the template D0, the consecutive guanine bases might induce formation of G-quadruplex motifs in the template^[16] and C-quadruplex/i-motif structures^[17] in the amplified RCA product may also contribute to the low RCA efficiency.

We note here that the amplification efficiency was highly reproducible, as determined by analyzing RCA product formation using different batches of polymerase and template sequences (Figure S8). Although the data did not allow establishing a direct link between DNA sequence and material properties, comparing D3a and D3b revealed that the formation of intra- and intermolecular interactions had a stronger effect on viscosity than the amount of present polymer chains alone.

Next, to investigate the effects of varying individual parameters, we chose template D2 due to this purest cyclization product, robust DNA yield and predictable secondary structure with a single predicted folding option for the amplicons (Table 1 and Figure S2). First, the influence of primer and template concentrations was investigated (Figure 3) by decreasing the primer concentration in 1:5 dilution steps from the concentrations specified in the two protocols of 667 nM and 100 nM for the Tan protocol and the Walther protocol, respectively. As shown in Figures 3A and B, the reduction in primer concentration under both conditions had minimal effect on the amount of formed RCA product. This result could additionally be attributed to short DNA oligonucleotides carried over from the exonuclease treatment and purification, which are not visible in the Urea-PAGE, but may nevertheless act as primers. It is known from the amplification of whole genomes that even hexamer oligonucleotides are sufficient to enable efficient RCA.^[18]

To investigate the influence of the template concentration, the initial concentrations of 400 nM and 50 nM set in the Tan and Walther protocols, respectively, were also reduced in 1:5 dilution steps (Figures 3C, D). Both protocols showed a clear decrease in product formation with decreasing template concentration (filled bars). In the case of the Tan protocol, the apparent viscosity of the hydrogels also decreased with decreasing amount of product (Figures 3A, C), whereas under Walther conditions only very low viscosities were obtained, which hardly showed such a positive correlation to primer and template concentration (Figures 3B, D). In fact, the measured

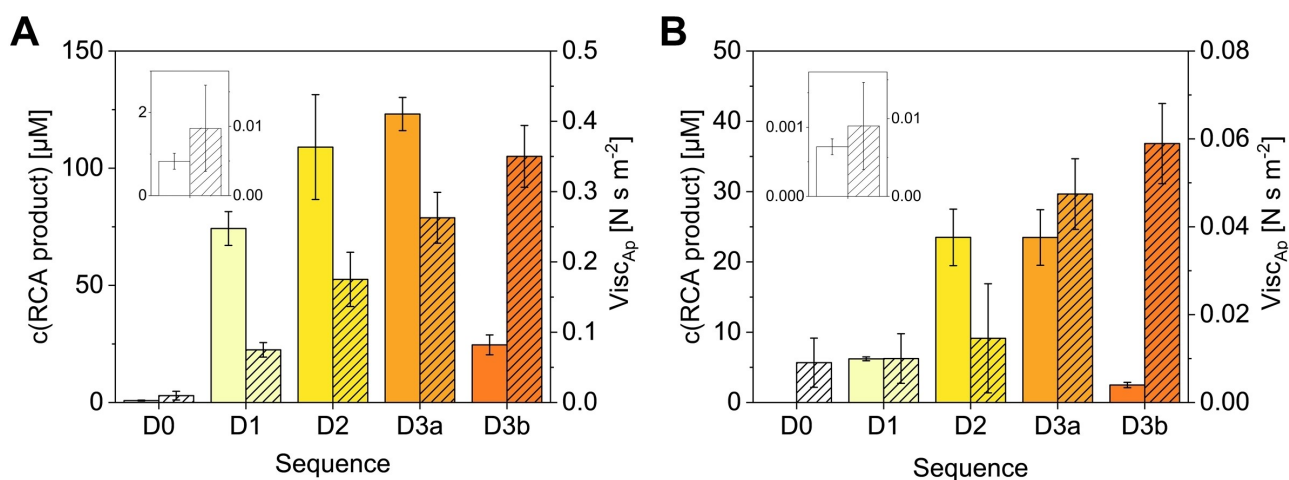


Figure 2. Analysis of RCA-based DNA hydrogels originating from various sequences D amplified by using RCA protocols of Tan (A) or Walther (B). RCA product concentration (filled bars) and apparent viscosity ($Visc_{Ap}$, hatched bars) were determined by qPCR and micromechanical indentation, respectively. All measurements were conducted as experimental triplicates and plotted as mean \pm standard deviation. Note the differently scaled y-axis.

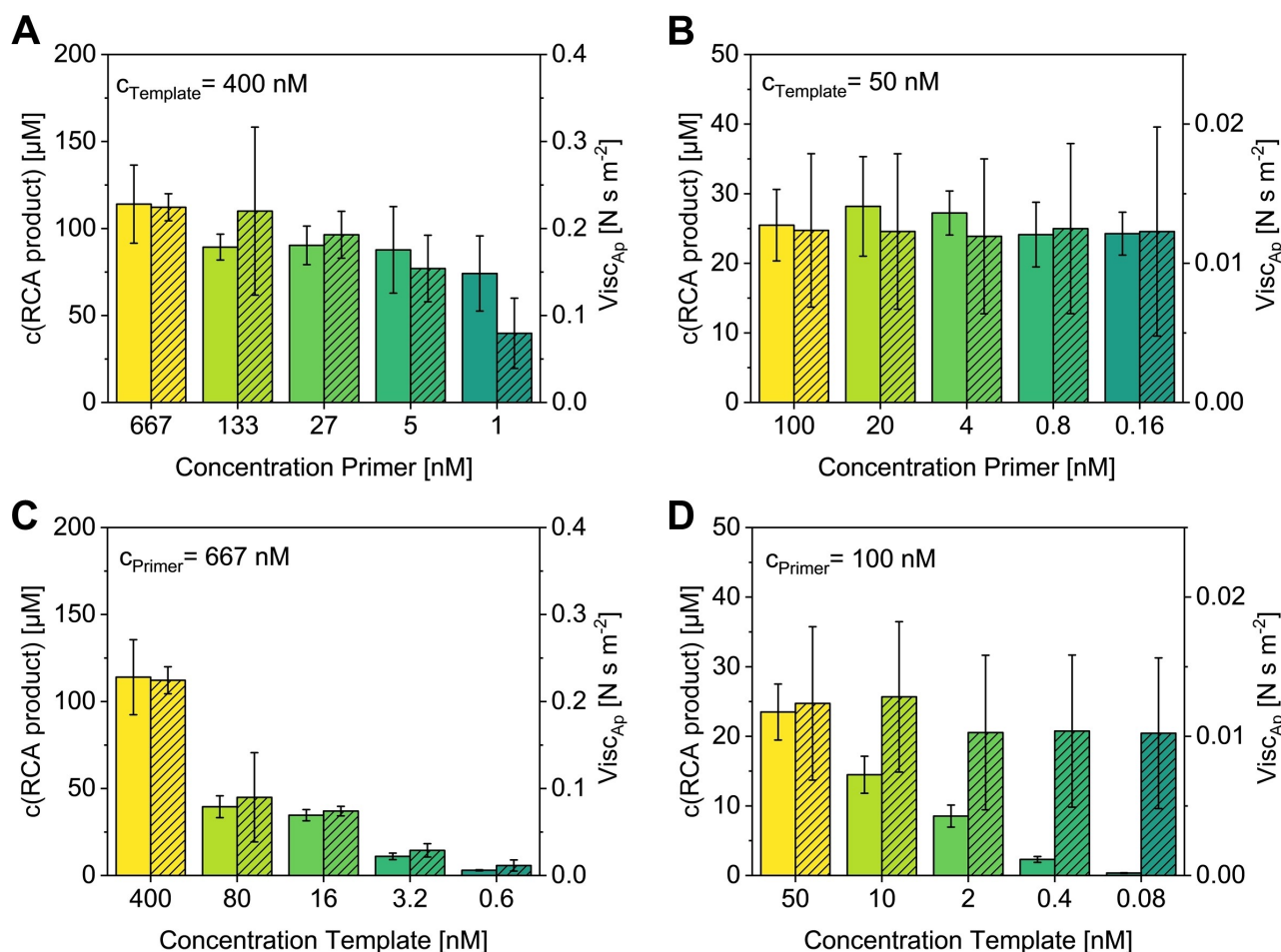


Figure 3. Influence of primer and template concentration on the amount and viscosity of DNA hydrogels formed from template D2 amplified by using RCA protocols of Tan (A, C) or Walther (B, D). RCA product concentration (filled bars) and apparent viscosity (Visc_{Ap} , hatched bars) were determined by qPCR and micromechanical indentation, respectively. All measurements were conducted as experimental triplicates and plotted as mean \pm standard deviation. Note the differently scaled y-axes. Also note that the equal distances on the x-axis in the bar graph do not reflect the 5-fold dilutions of the reagent concentration, which are better recognizable in symbol-line diagrams (Figure S10). For additional analysis by electrophoresis, see Figure S11.

viscosities were similar to the negative controls lacking polymerase showing an apparent viscosity of 0.01 N s m^{-2} (Figure S9).

The influence of the dNTP composition and concentration on the RCA process was then investigated. Although the final concentration in both cases is 5 mM, in contrast to the Tan protocol, the Walther protocol employs a sequence composition-adjusted dNTP mixture. Template sequence D2 contains about five times more thymine than adenine nucleotides. To evaluate the effects of dNTP composition and concentration, equimolar and adjusted dNTP mixtures at concentrations of 10, 5, 2.5, and 1.3 mM were used for hydrogel production. Using the Tan protocol (Figures 4A, C), we observed a clear dependence on the dNTP concentration. Higher dNTP concentrations (10 mM) led to increased RCA product formation, resulting in an approximately 1.6-fold increase with the adjusted dNTP mixture compared to the equimolar mixture. This observation highlights the usefulness of customized dNTP mixtures at high amplification rates, where the individual building blocks can be the limiting factor. The RCA hydrogels synthesized using the

Walther protocol (Figure 4B, D) also exhibited higher RCA product concentrations and apparent viscosity with increasing dNTP concentration. However, the influence of dNTP composition was less pronounced with the Walther protocol than with the Tan protocol, an observation consistent with the hypothesis that at lower synthesis rates the nature of the individual nucleotide building blocks plays less of a pivotal role.

We also investigated the influence of phi29 polymerase concentration on the RCA process by using variable concentrations of the enzyme from 1.0 to 0.1 U/ μL . For samples synthesized with the Tan protocol (Figure 5A), a clear positive correlation of product concentration with phi29 polymerase concentration was observed over the entire variation range, whereas with the Walther protocol this positive correlation only started at phi29 concentrations of $< 0.4 \text{ U}/\mu\text{L}$ (Figure 5B). These observations are also consistent with the hypothesis that low intrinsic synthesis rates are associated with this protocol, so that even an increased amount of catalyst (here $> 0.4 \text{ U}/\mu\text{L}$) has little influence.

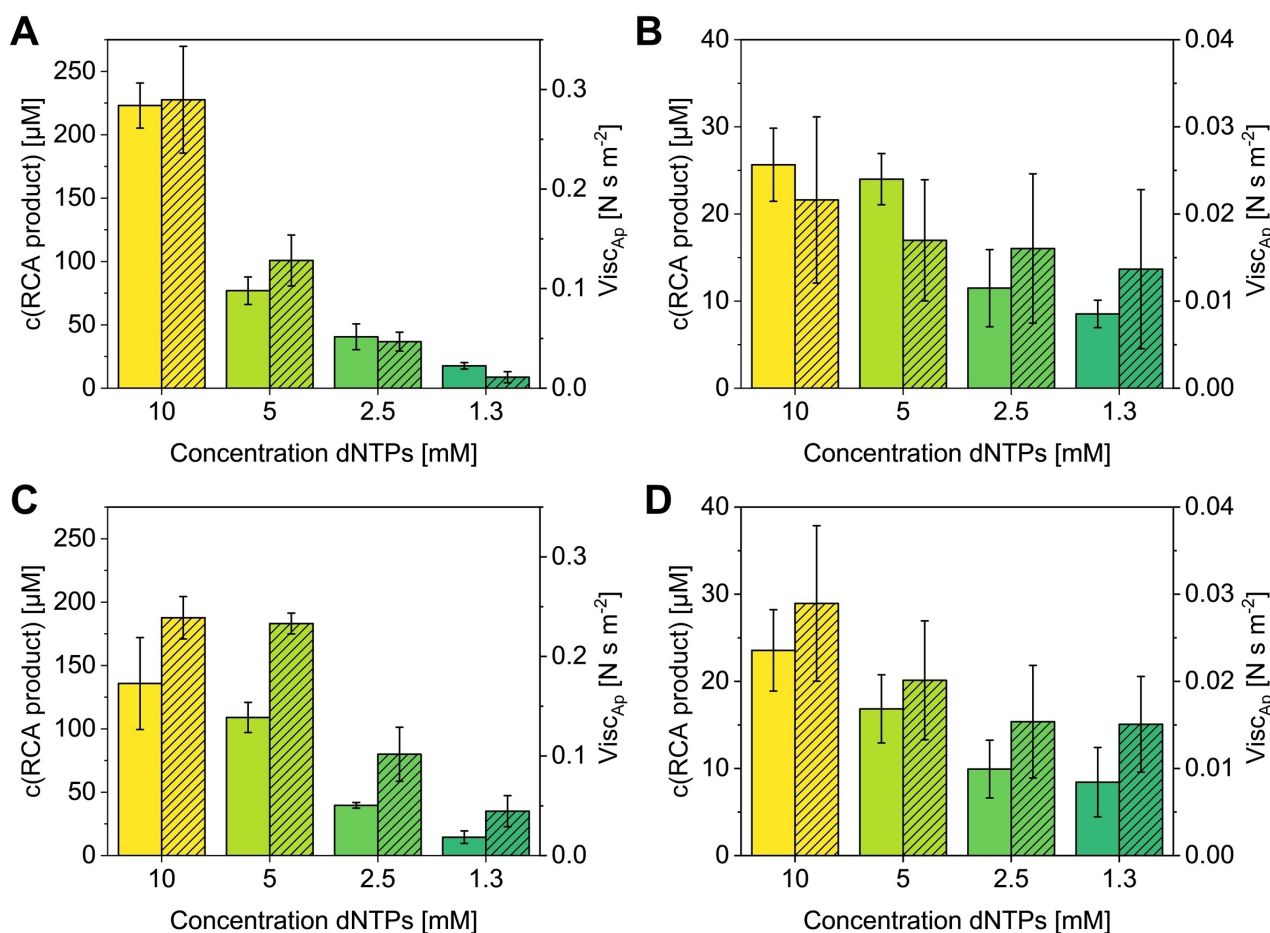


Figure 4. Influence of dNTP concentration and composition on the amount and viscosity of DNA hydrogels formed by RCA using template D2. Protocols of Tan (A,C) or Walther (B, D) were carried out with dNTP mix containing either sequence-adjusted (A, B) or equimolar (C, D) amounts of the four nucleotides. RCA product concentration (filled bars) and apparent viscosity ($Visc_{Ap}$, hatched bars) were determined by qPCR and micromechanical indentation, respectively. All measurements were conducted as experimental triplicates and plotted as mean \pm standard deviation. Note the differently scaled y-axes. Also note that the equal distances on the x-axes in the bar graph do not reflect the 2-fold dilutions of the reagent concentration, which are better recognizable in symbol-line diagrams (Figure S12). For additional analysis by electrophoresis, see Figure S13.

Bovine serum albumin (BSA) is used in the Tan protocol at a final concentration of 0.067 mg/mL as an additive to the RCA to stabilize the polymerase and prevent non-specific binding to vessel walls, which in turn can inactivate the enzyme. In contrast, the Walther protocol does not use BSA. To analyze possible effects of BSA, we ran both synthesis protocols with and without BSA (Figures 5C, D), while all other parameters were fixed at standard conditions (Figure 1). In the case of the Tan protocol (Figure 5C), we found no statistically significant differences (p -value: 0.471) between the samples with or without BSA.

However, a statistically significant difference (p -value: 0.011) was found for the samples synthesized according to the Walther protocol (Figure 5D). This is likely due to the rather low concentration of phi29 polymerase of 0.2 U/ μ L, at which the above-mentioned protective effects of the BSA additive are more pronounced than with the 0.67 U/ μ L polymerase concentration used in the Tan protocol.

Moreover, the utilization of low polymerase concentration in the Walther protocol, coupled with the addition of BSA,

appeared to hinder polymerase denaturation and subsequently led to a significant increase in RCA product formation. This observation underscores the intricate interplay between reaction components and may offer in future experiments a boost to the polymerization efficiency with an inexpensive additive. The hydrogels synthesized according to the Tan protocol exhibited a significant about 4-fold higher concentration of RCA product (for a statistical analysis of the values obtained for sequence D2, see Figure S17). Our findings also indicated that the Tan protocol has a stronger dependency on dNTP composition and concentration as well as on polymerase concentration than the Walther protocol, which is likely attributed to the higher amplification rate. Hence, lower amplification efficiency makes the Walther protocol somewhat more robust to variations in primer, nucleotide and polymerase concentrations.

Finally, we wanted to gain insight into the dependence of the materials property (apparent viscosity) on the RCA product concentration. Since the comparison of hydrogels prepared from different sequences and with different protocols could

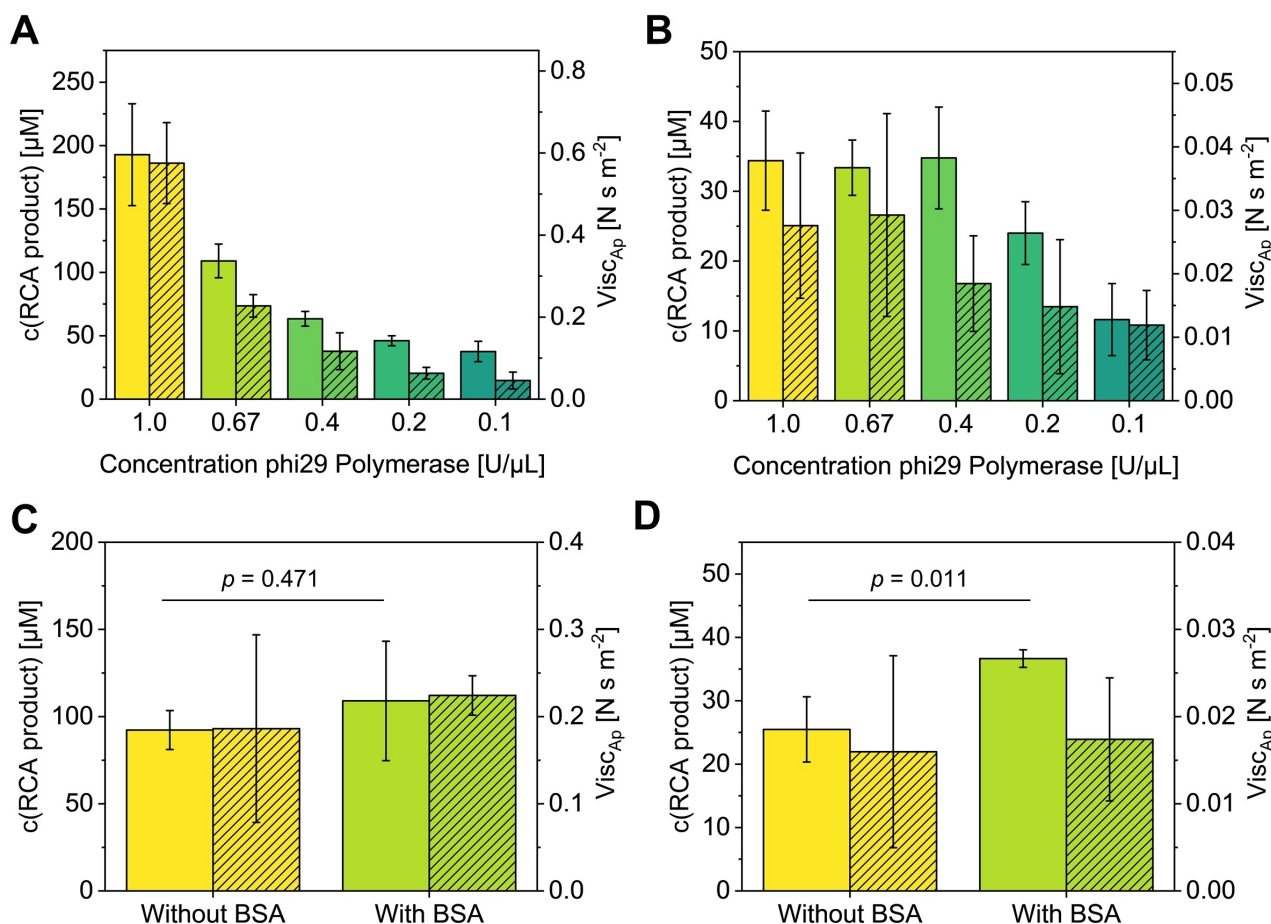


Figure 5. Influence of phi29 polymerase concentration and bovine serum albumin (BSA) addition on the amount and viscosity of DNA hydrogels formed by RCA of template D2, following the protocols of Tan (A, C) or Walther (B, D). RCA product concentration (filled bars) and mechanical properties (apparent viscosity ($Visc_{Ap}$), hatched bars) were determined by qPCR and micromechanical indentation, respectively. Note the differently scaled y-axes. Also note that the equal distances on the x-axes in the bar graph do not reflect the 66% dilutions of the polymerase concentration, which are better recognizable in symbol-line diagrams (Figure S14). All measurements were conducted as experimental triplicates and plotted as mean \pm standard deviation. For the statistical analysis two-tailed Student's t-test was used and a value of 0.05 was set as the significance level. For additional electrophoretic analyses, see Figures S15, S16.

show positive or negative correlations (positive: A, B, C with Walther, D0–D3a with Walther and Tan; negative: A, B, C with Tan, D3a – D3b with Walther and Tan), we hypothesize that both the amount of DNA and the amount of secondary structures play a crucial role and exert a combined effect on the mechanical properties. However, the specific conditions under which one factor dominates over the other are unclear. If the same DNA sequence is used to prepare hydrogels containing different amounts of DNA, the influence of secondary structures should be negligible, so that the relationship between viscosity and DNA concentration can be specifically investigated. To this end, we considered the viscosity and RCA product concentration data obtained with sequence D2 using the Tan protocol, as these showed a wider range of viscosities and concentrations than those generated with the Walther protocol. Since it is known that an exponential relationship exists between viscosity and DNA concentration for other types of hydrogels and also for DNA hydrogels prepared by hybridization of small building blocks, we fitted our data with the power-law of functional form $Visc_{Ap} = Visc_{Water} + A \cdot c^B$, as previously described.^[19]

As shown in Figure 6A, we found an exponential relationship between apparent viscosity and DNA concentration for the RCA hydrogel D2. Finally, to investigate whether this relationship also exists for other sequences, we used the template sequences D3a and D3b, as they revealed the highest apparent viscosities. To generate different concentrations of the RCA product, we used the Tan protocol with variable concentrations of the template (400–0.6 nM), as this parameter had the greatest effect on the RCA product concentration for sequence D2 (see Figure 3C). The experimental data of this study of hydrogels D3a and D3b are shown in Figure S18. The dependence of apparent viscosity on DNA concentration is shown in Figures 6B and 6C, respectively. Exponential correlation with a high coefficient of determination ($R^2 > 0.98$) was found for both.

Conclusions

The results obtained allow evaluating the robustness of the employed protocols to variations of each reagent parameter.

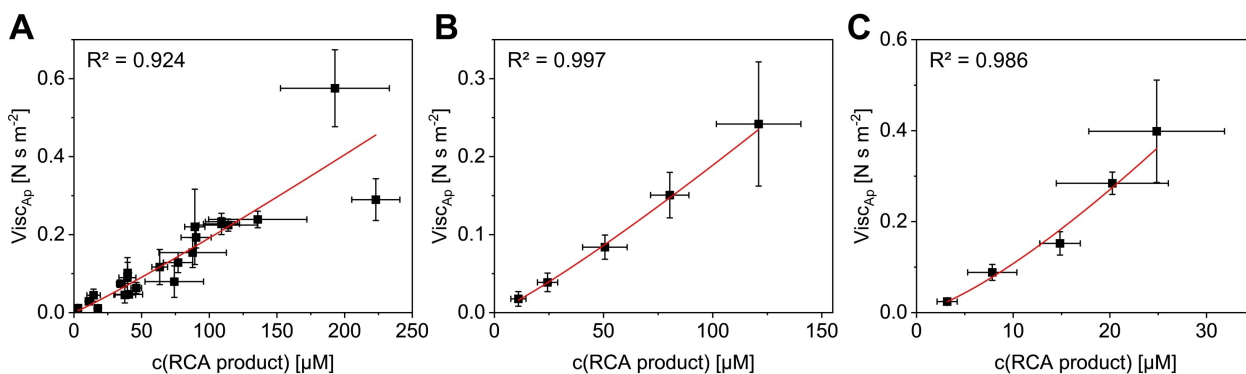


Figure 6. Investigation of the relationship between apparent viscosity and RCA product concentration. As previously described in the literature for other DNA hydrogels, an exponential relationship between the apparent viscosity and the RCA product concentration can be demonstrated for hydrogels with the sequence D2 (A), D3a (B) and D3b (C). The data in (A), obtained from sequence D2, corresponds to all apparent viscosities and RCA product concentrations obtained from the variation studies (Figures 3A, 3C, 4A, 4C, 5A). For sequences D3a (A) and D3b (C), the template concentration was varied from 0.6 to 400 nM using the Tan protocol in order to obtain different RCA product concentrations and, thus, apparent viscosities (see Figures S18, S19). Note the differently scaled y- and x-axes. All measurements were conducted as experimental triplicates and plotted as mean \pm standard deviation.

For an estimation, the numerical ratio of RCA product concentrations of template D2 obtained with the highest and lowest concentration of each variation, respectively, were calculated (Table S4). Consistently, variation in primer concentration and addition of BSA had the smallest effect for both protocols (approximately 1.3-fold). Variations in enzyme and nucleotide concentrations played a larger role (approx. 3–12-fold), in particular for the Tan protocol. However, the template concentration had the greatest influence on the productivity of the RCA (about 40- and 60-fold for the Tan and Walther protocols, respectively). Even this simple consideration underscores the need for high-quality circular RCA template, the preparation, purification and characterization of which remains one of the challenging aspects of protocol-specific optimizations.^[20]

With regards to the mechanical properties of the materials prepared in this study under reagent parameter variation (Figures 3–6), we confirmed the exponential correlation between concentration of DNA amplicon concatemers and apparent viscosity of the corresponding hydrogels. This result emphasizes the importance of absolute quantification of the amount of amplicons for rational design of DNA hydrogel materials, since clearly that the amount of polymer chains in a polymer suspension significantly affects its material properties, such as viscosity. In addition, the exact quantification plays a decisive role in the further use of DNA hydrogel materials, for example to deploy them for further functionalization into hybrid materials. In this context, it is crucial to adjust the ratio of biomolecules or any other components to the DNA carrier material to achieve optimal application-relevant properties. This control enables functionalization with proteins for biocatalytic use or with fluorophores and nanoparticles for sensory purposes.

While the material properties of DNA hydrogels depend to a first approximation on the polymer concentration, the nucleobase sequence plays an even more important role in these complex materials. This is particularly well exemplified by the sequence variations of template D0–D3a investigated here.

Here, dramatic differences in the amplification efficiency and the viscoelastic properties of the corresponding DNA materials were achieved with identical GC content through slight changes in the base sequence (Figure 2). Contrary to expectations, the presence of secondary structures led to improved synthesis performance and higher viscosities. Of particular importance is the comparison of the materials D3a and D3b, where almost identical base ratios and numbers of base-paired hairpin structures in the template resulted in very different DNA contents and material properties.

These findings prompt the search for further understanding of structure-property relationships of the DNA hydrogel materials. As one example, machine learning could be used to predict DNA sequences and process parameters for polymerization in order to produce DNA materials with defined mechanical properties - a task that is currently unfeasible. In the field of machine learning and artificial intelligence, it is crucial to have large, high-quality data sets to train neural networks and use them for predictions. We believe that the methodology presented here of combining high-throughput analytical methods to quantify polymer content and material properties with the modeling of sequence-dependent structural properties should help to obtain the necessary datasets.

Experimental Section

Synthesis of DNA Hydrogels

To enable RCA, the linear templates were first circularized. All sequences of the templates and primers are listed in Table S2. The template and primers were mixed at a final concentration of 5 μM each in 1x TE buffer (20 mM Tris-HCl, 1 mM EDTA, pH 7.6) with a final NaCl concentration of 100 mM. The DNA was hybridized at 25 °C and 400 rpm for 1.5 h. Then 20 μL of 10x commercial ligase buffer (New England Biolabs, USA, 500 mM Tris-HCl, 100 mM MgCl_2 , 100 mM dithiothreitol, and 10 mM ATP, pH 7.6), 78 μL of ddH₂O, and 2 μL of T4 ligase (400,000 U/mL, New England Biolabs, USA) were added into a tube containing 100 μL of the template strand,

gently mixed, and allowed to react at 25 °C for 3 h. The ligase was then deactivated by heating at 70 °C for 20 min.

To 200 μL of the ligation mixture, 23 μL of 10x NEB Puffer 1 (New England Biolabs, USA, 100 mM Bis-Tris-Propane-HCl, 100 mM MgCl_2 , 10 mM dithiothreitol, pH 7), 4 μL of exonuclease I (20,000 U/mL, New England Biolabs, USA) and 4 μL of exonuclease III (100,000 U/mL, New England Biolabs, USA) were added and the mixture was incubated at 37 °C overnight to digest primers and non-circularized templates. The enzymes were then deactivated by heating at 95 °C for 10 min. The circularized templates were purified by filtration through Vivacon ultracentrifugal filters with a 10 kDa cut-off (Satorius, Germany) and washed five times with 0.1x TE buffer. The template concentrations were determined using a Synergy plate reader (BioTek, USA), and the solutions were diluted to 1 μM with 0.1x TE buffer.

The circularization was analyzed with 10% Urea-PAGE. For two gels, 5 g Urea (Sigma-Aldrich, USA) were mixed with 2.4 mL 5x TBE (89 mM Tris base, 89 mM boric acid, 2 mM EDTA, pH: 8.0) and 6.6 mL ddH_2O . After sonication in an ultrasonic bath, 3 mL Acrylamide: Bisacrylamide (29:1, Sigma Aldrich, USA), 100 μL 10% (w/v) APS (Sigma-Aldrich, USA) and 10 μL TEMED (Sigma-Aldrich, USA) were added and the gels were polymerized for 1 h. Novex™ TBE-Urea Sample Buffer (2x) (ThermoFischer, Germany) was added to the samples and the gels were run at 70 V for 1.5 h. The DNA was stained by the addition of 3 μL SYBR Gold (ThermoFischer, Germany) in 50 mL 1x TBE and captured with a gel reader (Fusion FX, Vilber, Germany, software: Evolution-Capt Edge). For a representative gel image of the ligated samples, see Figure S3B.

For a RCA batch of 75 μL synthesized following the Tan protocol,^[7] 30 μL 1 μM circularized template, 5 μL 10 μM primer, 10 μL 10 mM dNTPs (New England Biolabs, USA), 5 μL 10x phi29 reaction buffer (New England Biolabs, USA: 500 mM Tris-HCl, 10 mM MgCl_2 , 100 mM $(\text{NH}_4)_2\text{SO}_4$, 40 mM dithiothreitol, pH 7.5), 5 μL 1 mg/mL albumin, 15 μL ddH_2O and 5 μL phi29 polymerase (10,000 U/mL, New England Biolabs, USA) were mixed. The RCA mixture was incubated at 30 °C for 72 h.

To synthesize RCA hydrogels according to the Walther protocol,^[6] a 250 μL reaction mixture was prepared from 192.5 μL of ddH_2O , 12.5 μL of a 1 μM circular DNA template, 25 μL of 10x phi29 reaction buffer, 2.5 μL of a 10 μM RCA primer and 5 μL of the phi29 polymerase were mixed. Subsequently, 12.5 μL of a dNTP solution (100 mM, adjusted to the base composition of the amplicon sequence) was added. The specific ratio of dNTPs was for Template A: 12:16:26:18 (A:T:G:C), Template B: 9:16:23:24 (A:T:G:C), Template C: 22:21:23:27 (A:T:G:C), Template D0: 8:30:58:0 (A:T:G:C), Template D1: 6:32:47:11 (A:T:G:C), Template D2: 32:6:29:29 (A:T:G:C), Template D3a: 27:11:27:31 (A:T:G:C), Template D3b: 28:10:30:28 (A:T:G:C). The RCA reaction was incubated at 30 °C for 72 h. A tabular overview of the composition of the synthesis protocols can be found in Table S1, a detailed overview of the final concentrations of the varied conditions is given in Table S3.

Secondary Structure Analysis

The prediction of the secondary structures of the circularized templates and for one or four units of the RCA amplicons produced by means of templates A–D was performed using the mfold web server, based on free energy calculations and all designed templates.^[11]

Circular Dichroism Spectroscopy

All samples were measured with a concentration of 1 μM in 0.1x TE buffer, using a Jasco, J-1500 circular dichroism spectrometer. Parameters: measurement wavelength range 200–350 nm, data interval 1 nm, scanning speed 100 nm/min, bandwidth 4 nm. Scans were repeated 3 times for each sample (3 accumulations).

Quantification of RCA Products by qPCR

The quantification of the RCA product concentration was performed by qPCR using a previously established method by Schneider et al.^[5b] The used primer and probes can be found in Table S2. In brief, specific qPCR calibration curves were first generated for each circular template. The calibration curve ranged from 20 nM to 156.3 pM. For representative calibration curves see Figure S6. For the various hydrogel samples, the reaction of a 10 μL aliquot was terminated following the addition of 90 μL of water by incubation at 80 °C for 10 min. Dilutions (1:4000–1:16000) were then prepared for qPCR measurements by thorough mixing and treatment with ultrasound for 5 s to fragment the DNA concatemers. To prepare a 10 mL qPCR mix, 1 mL of 10x qPCR buffer (160 mM $(\text{NH}_4)_2\text{SO}_4$, 670 mM Tris-HCl, 25 mM KCl, 25 mM MgCl_2 , 0.1% (v/v) Tween-20), along with 200 μL of 10 mM dNTPs each, 100 μL each of 100 μM forward and reverse primers, 20 μL of 100 μM probe, and 100 μL of Taq DNA polymerase (5,000 U/mL, New England Biolabs, USA) were combined in autoclaved ddH_2O . For qPCR analysis, 20 μL of the qPCR mix were mixed with 1.5 μL of either the sample (i.e., calibration standards or RCA samples). The measurements were conducted in technical triplicates using a real-time thermocycler from Corbett Research (Australia). The cycle threshold (Ct) value was subtracted from the maximum number of cycles (C_{max}). DNA concentrations were obtained using linear regression by plotting the resulting ΔCt values against the logarithmic concentration of the calibration standards. The qPCR quantification of RCA samples was performed in at least three independent experiments.

Agarose Gel Electrophoresis

For the analysis of the formation of RCA product, the hydrogel precursor mixtures were mixed as previously described and aliquoted to 5 μL . The RCA reaction was quenched by heating for 10 min at 95 °C. The samples were analyzed on a 1% agarose gel at 140 V for 60 min. GeneRuler™ 1 kb DNA (ThermoFischer, Germany) was used as a ladder. For representative gel images, see Figures S6, S11, S13, S15, S16 and S19.

Rotational Rheometry

To characterize DNA hydrogels, a rotational rheometer (Physica MCR 501, Anton Paar, Germany) equipped with a cone-and-plate (diameter 50 mm, cone-angle 1°) measuring cell was used to perform small amplitude oscillatory shear experiments. Strain sweep experiments performed prior to frequency sweeps ensured that the strain amplitude was sufficiently low to provide a linear material response. For frequency sweep tests, the frequency range covered was from 0.05 to 15 Hz. From these curves, the value of the elastic modulus G_0 at a frequency of 0.2 Hz was recorded, where the former exhibits a plateau.

Viscosity Measurements with In-House Developed Indentation Platform

For rapid analysis of the apparent viscosity of the RCA product samples, an in-house developed indentation platform was used.^[10] The system is based on an indentation probe equipped with micrometer drive actuators that allows the quantitative determination of viscosity for exceptionally soft and viscous hydrogels. To this end, the indentation probe, a plunger measuring 18 mm in length, 4.3 mm in diameter, is used to displace the viscous sample in the sample container (4.5 mm diameter cavity, 4 mm depth). The plunger is attached to a calibrated load cell that measures the force needed for indentation and displacement of the sample in/from the sample container. For the determination of the apparent viscosity of DNA hydrogels, the device was calibrated with water, glycerol and water-glycerol mixtures at 25 °C.^[10]

Statistical Analysis

The average values and error bars were analyzed from at least triplicate measurements ($n=3$) and expressed as mean \pm standard deviation. Origin 2019 software (OriginLab, USA) was used for data analysis and visualization. Statistical analysis was performed using two-tailed Student's t-test or one-way ANOVA for multiple samples with Tukey post hoc tests for pairwise comparisons. All analyses were performed using SPSS statistical package 29.0 (IBM, USA). A p -value of 0.05 was set as the significance level.

Supporting Information Summary

Additional supporting information can be found online in the Supporting Information section at the end of this article.

Acknowledgements

This work was financially supported through the Helmholtz Association program "Materials Systems Engineering" under the topic "Adaptive and Bioinspired Materials Systems". Svenja Moench is grateful for a Kekulé fellowship by Fonds der Chemischen Industrie (FCI). We thank Stefan Heissler (IFG, KIT) for help with the CD spectroscopy. Open Access funding enabled and organized by Projekt DEAL.

Conflict of Interests

The authors declare no conflict of interest.

Data Availability Statement

The data that support the findings of this study are available from the corresponding author upon reasonable request.

Keywords: DNA · DNA hydrogels · Gels · Rolling circle amplification · Viscosity

- [1] a) Y. Dong, C. Yao, Y. Zhu, L. Yang, D. Luo, D. Yang, *Chem. Rev.* **2020**, *120*, 9420–9481; b) D. Wang, Y. Hu, P. Liu, D. Luo, *Acc. Chem. Res.* **2017**, *50*, 733–739; c) M. Vázquez-González, I. Willner, *Angew. Chem. Int. Ed. Engl.* **2020**, *59*, 15342–15377; d) V. Morya, S. Walia, B. B. Mandal, C. Ghoroi, D. Bhatia, *ACS Biomater. Sci. Eng.* **2020**, *6*, 6021–6035.
- [2] a) R. Hu, X. Zhang, Z. Zhao, G. Zhu, T. Chen, T. Fu, W. Tan, *Angew. Chem., Int. Ed.* **2014**, *126*, 5931–5936; b) J. Li, L. Mo, C.-H. Lu, T. Fu, H.-H. Yang, W. Tan, *Chem. Soc. Rev.* **2016**, *45*, 1410–1431; c) E. Kim, L. Zwi-Dantsis, N. Reznikov, C. S. Hansel, S. Agarwal, M. M. Stevens, *Adv. Mater.* **2017**, *29*, 1701086; d) Y. Wang, E. Kim, Y. Lin, N. Kim, W. Kit-Anan, S. Gopal, S. Agarwal, P. D. Howes, M. M. Stevens, *ACS Appl. Mater. Interfaces* **2019**, *11*, 22932–22940.
- [3] L. Blanco, A. Bernad, J. M. Lázaro, G. Martín, C. Garmendia, M. Salas, *J. Biol. Chem.* **1989**, *264*, 8935–8940.
- [4] Y.-p. Gao, K.-J. Huang, F.-T. Wang, Y.-Y. Hou, J. Xu, G. Li, *Analyst* **2022**, *147*, 3396–3414.
- [5] a) B. Joffroy, Y. O. Uca, D. Prešern, J. P. K. Doye, T. L. Schmidt, *Nucleic Acids Res.* **2018**, *46*, 538–545; b) L. Schneider, R. Richter, C. Oelschlaeger, K. S. Rabe, C. M. Domínguez, C. M. Niemeyer, *Chem. Commun.* **2023**, *59*, 12184–12187.
- [6] R. Merindol, G. Delechiave, L. Heinen, L. H. Catalani, A. Walther, *Nat. Commun.* **2019**, *10*, 528.
- [7] G. Zhu, R. Hu, Z. Zhao, Z. Chen, X. Zhang, W. Tan, *J. Am. Chem. Soc.* **2013**, *135*, 16438–16445.
- [8] a) Y. Hu, C. M. Domínguez, J. Bauer, S. Weigel, A. Schipperges, C. Oelschlaeger, N. Willenbacher, S. Keppler, M. Bastmeyer, S. Heißler, C. Wöll, T. Scharnweber, K. S. Rabe, C. M. Niemeyer, *Nat. Commun.* **2019**, *10*, 5522; b) Y. Hu, C. M. Niemeyer, *J. Mater. Chem. B* **2020**, *8*, 2250–2255; c) Y. Hu, D. Rehnlund, E. Klein, J. Gescher, C. M. Niemeyer, *ACS Appl. Mater. Interfaces* **2020**, *12*, 14806–14813.
- [9] C. Liu, J. He, E. v. Ruymbeke, R. Keunings, C. Bailly, *Polymer* **2006**, *47*, 4461–4479.
- [10] P. Lemke, S. Moench, P. S. Jäger, C. Oelschlaeger, K. S. Rabe, C. M. Domínguez, C. M. Niemeyer, *Small Methods* **2024**, 2400251.
- [11] M. Zuker, *Nucleic Acids Res.* **2003**, *31*, 3406–3415.
- [12] O. Doluca, J. M. Withers, V. V. Filichev, *Chem. Rev.* **2013**, *113*, 3044–3083.
- [13] J. Kyrp, I. Kejnovská, D. Renčiu, M. Vorličková, *Nucleic Acids Res.* **2009**, *37*, 1713–1725.
- [14] a) T. C. Davenport, *Phys. Educ.* **1968**, *3*, 139; b) S. Thammakiti, M. Suphantharika, T. Phaesuswan, C. Verduyn, *Int. J. Food Sci. Technol.* **2004**, *39*, 21–29; c) F. J. Galindo-Rosales, F. J. Rubio-Hernández, A. Sevilla, *J. Non-Newton. Fluid Mech.* **2011**, *166*, 321–325.
- [15] a) M. a. S. Soengas, C. Gutiérrez, M. Salas, *J. Mol. Biol.* **1995**, *253*, 517–529; b) J. L. Montgomery, N. Rejali, C. T. Wittwer, *J. Mol. Diagnostics* **2014**, *16*, 305–313.
- [16] M. L. Bochman, K. Paeschke, V. A. Zakian, *Nat. Rev. Genet.* **2012**, *13*, 770–780.
- [17] H. Abou Assi, M. Garavis, C. González, M. J. Damha, *Nucleic Acids Res.* **2018**, *46*, 8038–8056.
- [18] R. Johne, H. Müller, A. Rector, M. van Ranst, H. Stevens, *Trends Microbiol.* **2009**, *17*, 205–211.
- [19] I. D. Stoev, T. Cao, A. Caciagli, J. Yu, C. Ness, R. Liu, R. Ghosh, T. O'Neill, D. Liu, E. Eiser, *Soft Matter* **2020**, *16*, 990–1001.
- [20] a) R. An, Q. Li, Y. Fan, J. Li, X. Pan, M. Komiyama, X. Liang, *Nucleic Acids Res.* **2017**, *45*, e139–e139; b) J. Chen, Y. R. Baker, A. Brown, A. H. El-Sagheer, T. Brown, *Chem. Sci.* **2018**, *9*, 8110–8120; c) Y. Cui, X. Han, R. An, G. Zhou, M. Komiyama, X. Liang, *RSC Adv.* **2018**, *8*, 18972–18979.

Manuscript received: May 7, 2024

Accepted manuscript online: July 12, 2024